



**HAL**  
open science

## Impact of Mobility Model on LoRaWan Performance

Abdelouahab Nouar, Mounir Tahar Abbes, Selma Boumerdassi, Mostefa Chaib

► **To cite this version:**

Abdelouahab Nouar, Mounir Tahar Abbes, Selma Boumerdassi, Mostefa Chaib. Impact of Mobility Model on LoRaWan Performance. Journal of Communications, 2024, pp.7-18. 10.12720/jcm.19.1.7-18. hal-04680645

**HAL Id: hal-04680645**

**<https://hal.science/hal-04680645v1>**

Submitted on 7 Oct 2024

**HAL** is a multi-disciplinary open access archive for the deposit and dissemination of scientific research documents, whether they are published or not. The documents may come from teaching and research institutions in France or abroad, or from public or private research centers.

L'archive ouverte pluridisciplinaire **HAL**, est destinée au dépôt et à la diffusion de documents scientifiques de niveau recherche, publiés ou non, émanant des établissements d'enseignement et de recherche français ou étrangers, des laboratoires publics ou privés.



Distributed under a Creative Commons Attribution - NonCommercial - NoDerivatives 4.0 International License

# Impact of Mobility Model on LoRaWAN Performance

Abdelouahab Nouar<sup>1</sup>, Mounir Tahar Abbes<sup>1,\*</sup>, Selma Boumerdassi<sup>2</sup>, and Mostefa Chaib<sup>1</sup>

<sup>1</sup>Department Science Computer, LME Laboratory, Hassiba Ben Bouali University, Chlef, Algeria

<sup>2</sup>CNAM/CEDRIC Laboratory, France

Email: a.nouar@univ-chlef.dz (A.N.); m.taharabbes@univ-chlef.dz (M.T.A.); m.chaib@univ-chlef.dz (M.C.);

selma.boumerdassi@cnam.fr (S.B.)

\*Corresponding author

**Abstract**—LoRaWAN (Long Range Wide Area Network) is a low-power wireless technology with an extended range. It is utilized frequently in Internet of Things (IoT) applications. Consequently, numerous IoT applications and solutions incorporate mobility. However, the increasing number of End Devices (ED) and mobility models of nodes impact the network performance of LoRaWAN (packet size, latency, energy consumption, and Packet Delivery Ratio (PDR)). This paper studies the influence of mobility models on the performance of LoRaWAN by using different scenarios under extensive simulations with the Network Simulator (NS3), including the random waypoint model, the Gauss Markov model, and the constant position model. The results indicate that the manner in which nodes move significantly impacts network performance; for instance, the Gauss-Markov model maintains a high level of network performance. To validate the simulation results, extensive experiments have been conducted with the Lora end device CubeCell HTCC-AB01 model in a variety of scenarios by analyzing the RSSI (Received Signal Strength Indicator) level in urban and rural areas using a large number of trajectories.

**Keywords**—LoRaWAN, NS3, LPWAN (low-power, wide-area networks), mobility model, RSSI, lora

## I. INTRODUCTION

LoRaWAN is a wireless communication protocol for Low-Power, Wide-Area Networks (LPWANs). One of the critical features of LoRaWAN is its ability to support long-range communications, making it well-suited for applications that require low-power, long-range connectivity. It is based on the LoRa (Long Range) modulation technology developed by Semtech Corporation. LoRaWAN uses a star network topology where end devices communicate with one or more Gateways (GW), which communicate with a Network Server (NS). The network server manages the communication between the end devices, and the application server provides the end-user interface and data processing [1], as shown in Fig. 1.

LoRaWAN uses the Adaptive Data Rate (ADR) algorithm to optimize transmission data rates for end

devices. The algorithm determines the optimal combinations of Spreading Factor (SF), bandwidth (BW), and Transmit Power (TP) of end devices to increase their transmission data rates, reduce their transmission airtime, and optimize their energy efficiency [2]. The network needs some measurements (uplink messages) to determine the optimal data rate. Currently, The Things Stack takes the 20 most recent uplinks, starting when the ADR bit is set. These measurements contain the frame counter, signal-to-noise ratio (SNR), and number of gateways that received each uplink.

For each of these measurements, take the SNR of the best gateway and calculate the so-called “margin,” which is the measured SNR minus the required SNR to demodulate a message given the data rate. This margin determines how much one can increase the data rate or lower the transmit power. One domain that can benefit from LoRaWAN’s mobility features is asset tracking. With LoRaWAN, tracking assets over long distances is possible, even in areas where traditional cellular networks are unavailable. For example, logistics companies can use LoRaWAN to track the location and condition of their shipments, allowing them to optimize their supply chain and improve efficiency. Another domain where LoRaWAN’s mobility features can be helpful in smart cities. With LoRaWAN, it is possible to collect data from many sensors deployed throughout a city, including traffic sensors, environmental sensors, and utility meters. These sensors are often outdoors and can be spread across a large area; LoRaWAN’s long-range communications and mobility features can help ensure reliable connectivity and data collection. LoRaWAN can also be used in the agriculture industry to track livestock or monitor environmental conditions, in the healthcare industry to track medical devices or patient health, and in the industrial sector to track inventory or monitor equipment health.

In the context of LoRaWAN, a mobility model refers to a mathematical model that describes the movement of nodes within a network. A mobility model can be used to simulate the behavior of nodes in a LoRaWAN network

and evaluate its performance under different scenarios. Using a mobility model to simulate the behavior of nodes in a LoRaWAN network makes it possible to assess the network's performance under other conditions.

This research focuses on the impact of three major mobility models: the Random Way Point (RWP) model, the Gauss Markov (GM) model, and the Constant Position (CP) model on the performance of LoRaWAN such as Energy Remaining, node density, PDR (Packet Delivery Ratio), delay and Packet size, this can be useful in optimizing the network design and improving its performance using network simulator NS3. Based on our bibliographic analysis of recent scientific publications, it has been observed that a significant number of authors engaged in research and simulations about the Lora network, extensively employed in industrial and academic domains, tend to overlook the incorporation of node movement parameters that will be simulated in mobility models within the context of this study. The significance of doing this scientific research is now evident, as it will focus on the specific parts requiring investigation and promptly illustrate the impact of these factors on the findings, resulting in substantial time savings.

The remaining sections are organized as follows: The Section II explains some fundamental concepts and performance metrics of LoRaWAN, including mobility patterns, PDR, Delay, and the energy framework. The related works are presented in Section III. Section IV illustrates the experiences, results under NS3, and discussion. Section V describes the experimental model configuration and presents findings and analysis. Section VI provides concluding remarks and a discussion of future work.

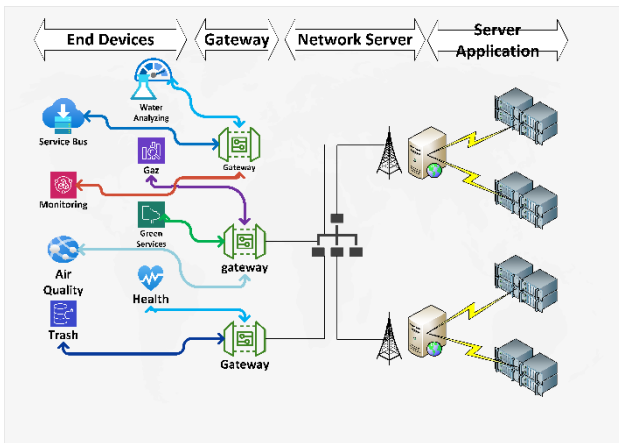


Fig. 1. LoraWan architecture.

## II. BACKGROUND LORAWAN

Any network must consider the mobility aspect. Nodes in WSNs (Wireless Sensors Network) can migrate anytime and in any direction. Network architecture can be damaged by high mobility, which can also be the reason for the odd behavior of network communication. Rapidly moving cluster heads could lead to the collapse of the entire cluster, squandering resources. Furthermore, repeated re-clustering consumes more energy. As a result, the sensor

node's mobility was taken into consideration. Random nodes were moved around the network to test mobility in the current system. Similar random selection is used to determine the node's new location. The mobility level of a node is determined by computing the difference between its previous and current positions.

Eq. (1) is used to determine the level of mobility [3].

$$ML = \sqrt{(x_{new} - x_{curr})^2 + (y_{new} - y_{curr})^2} \quad (1)$$

where  $(x_{new}, y_{new})$  are the coordinates of the sensor node at the new position and  $(x_{curr}, y_{curr})$  are the coordinates points of nodes at the last calculated position. An inverse relationship exists between a node's mobility and chances of becoming a cluster head; therefore, a node with a high mobility level has fewer chances to be selected as a cluster head.

### A. Mobility Patterns

The movement patterns of mobile elements are categorized by mobility models, which can be roughly divided into four subclasses as shown in Fig.2.: random mobility models: Random Waypoint (RWP), Random Walk (RW), Random direction (RD), models with temporal dependency: Gauss Markov (GM), Semi-Markov Smoot, models with spatial dependence: Probabilistic Random Walk, and models with geographic restriction: Pathway.

In this study, the RWP, GM, and Constant Position (CP) models are the three alternative mobility patterns to describe how the node moves.

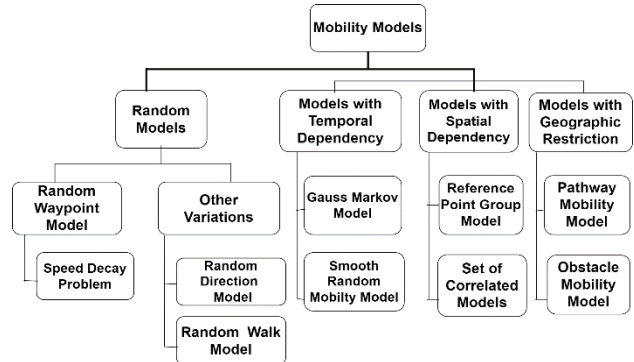


Fig. 2. Mobility models.

#### 1) Random waypoint mobility model (RWP)

Johnson and Maltz were the ones who first introduced the Random Waypoint mobility concept [4]. Because of its simplicity, it is the most frequently utilized for mobile ad hoc networks [5]. The Random Waypoint mobility model assigns each node a randomly distributed speed between  $[V_{min}, V_{max}]$  and a random destination inside the simulation zone.

The node stops at the destination for the time specified by the t pause parameter. Continual movement results if t pause=0. Upon expiration of this period, the node selects and moves toward a different random location within the simulation region. Until the simulation is over, the entire process is repeated numerous times[6], as shown in Fig. 3.

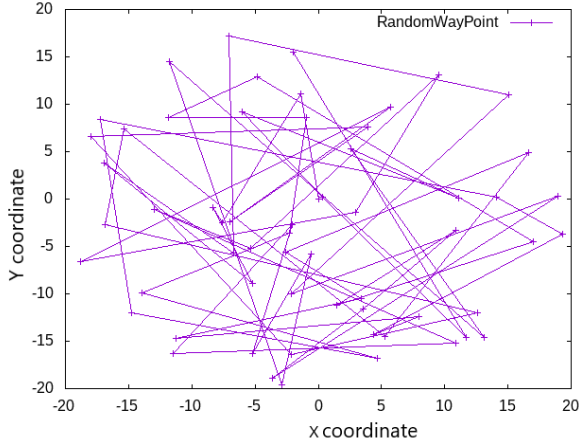


Fig. 3. Trajectory of end device under the random waypoint (RWP) model.

### 2) Gauss-markov mobility model (GM)

One tuning parameter [4, 5] allows the Gauss-Markov mobility model to adjust to various amounts of unpredictability. Each node is first given a current speed and direction. Nodes move by updating their respective speeds and directions at set intervals  $n$ . Specifically, this is achieved by determining the speed and direction at the  $n$ th instance based on the speed and direction at the  $(n-1)$  st instance and a random variable using the following equations:

$$v_n = \alpha v_{n-1} + (1 - \alpha)\bar{v} + \sqrt{1 - \alpha^2}v_{x_{n-1}} \quad (2)$$

$$d_n = \alpha d_{n-1} + (1 - \alpha)\bar{d} + \sqrt{1 - \alpha^2}d_{x_{n-1}} \quad (3)$$

where,

- $V_n$  and  $D_n$  are the new speed and direction of the node at time interval  $n$ .
- $\bar{v}$  and  $\bar{d}$  are constants representing the mean value of speed and direction as  $n \rightarrow \infty$ .
- $v_{x_{n-1}}$  and  $d_{x_{n-1}}$  are random variables from a Gaussian distribution.
- $\alpha$ , where  $0 \leq \alpha \leq 1$ , is the tuning parameter used to vary the randomness; very random values or Brownian motion is obtained by setting  $\alpha=0$  and linear motion is obtained by setting  $\alpha=1$ . Intermediate levels of randomness are obtained by varying the value of  $\alpha$  between 0 and 1.

At each time interval, the next location is calculated based on the current location, speed, and direction of movement. Specifically, at time interval  $n$ , a node's position is given by Eqs. (4–5):

$$x_{\{n\}} = x_{\{n-1\}} + v_{\{n-1\}} \text{Cos } d_{\{n-1\}} \quad (4)$$

$$y_{\{n\}} = y_{\{n-1\}} + v_{\{n-1\}} \text{Sin } d_{\{n-1\}} \quad (5)$$

where,  $(x_n, y_n)$  and  $(x_{n-1}, y_{n-1})$  are the  $x$  and  $y$  Coordinates for the node position at the  $n$ th and  $(n-1)$  time intervals, respectively, and  $(v_{n-1})$ ,  $(d_{n-1})$  are the speed and direction of the node, respectively, at the  $(n-1)$  time interval.

### 3) Gauss markov variables

**Alpha  $\alpha$ :** The variable  $\alpha$  is the tuning parameter for GM. Setting  $\alpha$  to a value between 0 and 1 allows us to adjust the degree of the model randomness. When  $\alpha=1$ , the model will be predictable and lose all of its randomness, and the new direction and velocity will be the same as the previous direction and velocity. Thus, when  $\alpha=1$ , the node moves in a straight line:

Fig. 4 shows an example of a GM trajectory in a 2D area. Linear motion is obtained by setting  $\alpha = 1$ .

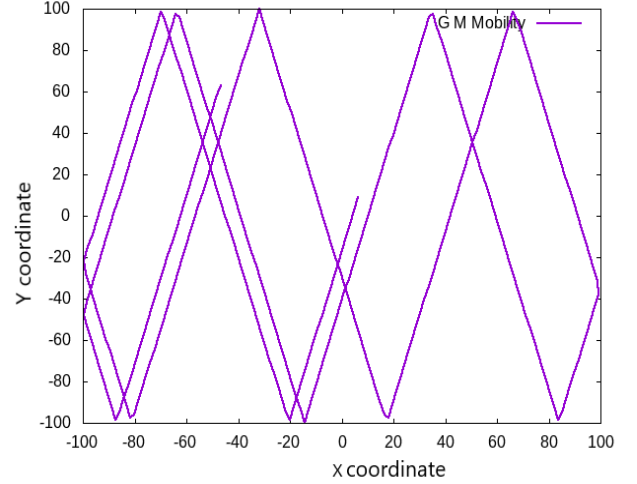


Fig. 4. G M Model, Alpha = 1.

On the other hand, when  $\alpha=0$ , the model will become memoryless, and the new direction and velocity will depend on the mean and standard deviation values of the direction and velocity and the Gaussian random variables.

Fig. 5 shows an example of a GM trajectory. A Brownian motion is obtained by setting  $\alpha = 0.5$ .

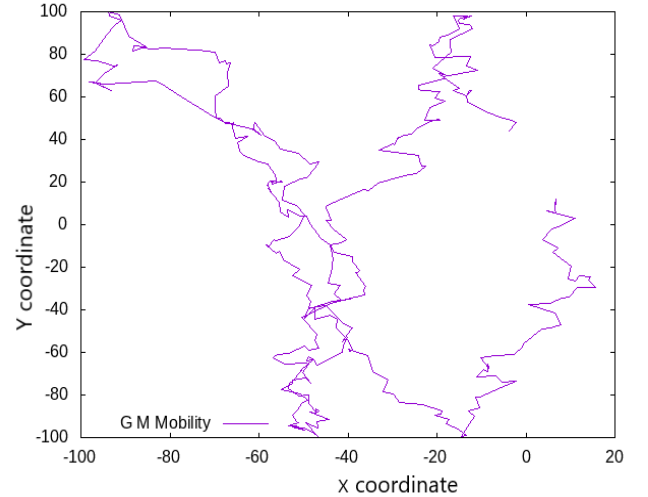


Fig. 5. G M Model, Alpha = 0.5.

### B. Energy Framework

Energy usage is a critical concern for wireless devices, and researchers in wireless networking often need to analyze the energy consumption of nodes or the overall network during network simulations using Ns-3 [7]. To facilitate this, Ns-3 must include support for energy

consumption modeling. Moreover, with the growing viability of concepts like fuel cells and energy scavenging for low-power wireless devices, it is essential to incorporate the impact of these emerging technologies into simulations by enabling the modeling of diverse energy sources in NS-3. Fig. 6. depicts the NS-3 Energy Framework, which is the foundation for modeling energy consumption, energy sources, and energy harvesting [8].

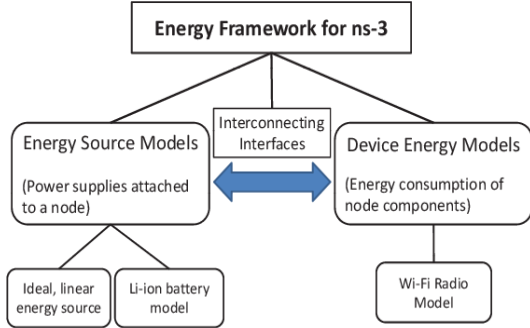


Fig. 6. Proposed ns-3 Energy Framework structure, including energy sources, device energy models, and interfaces [9].

### 1) Energy source

The Energy Source is a vital component of each node, serving as its power source. Multiple device energy models can be connected to each energy source, and a node may have more than one energy source. Once an energy source is linked to an energy model, it is assumed that that source powers the corresponding device. The Energy source's primary purpose is to provide power to the devices connected to the node. When the energy runs out, the devices are immediately informed and can take appropriate action. Energy source objects are also available to every node, offering beneficial data such as battery level and remaining energy. This feature is particularly advantageous for NS-3 when implementing energy-efficient protocols. The Energy Source needs to precisely reflect their practicality and effectiveness to simulate different power sources, like batteries, as they are vital features.

The Energy Source regularly surveys all the devices and energy harvesters within a given device to determine the combined current channel and energy consumption. When a node changes condition, the associated Device Energy Model will inform the Energy Source about this modification, potentially affecting the lifespan of a battery through two distinct effects. The first is the Rate Capacity Effect, which can reduce the battery's lifespan if the current draw exceeds its rated value. Conversely, the Recovery Effect can extend the battery's lifespan by cycling between discharge and idle states. In order to account for the Rate Capacity Effect, the Energy Source analyses and estimates the energy consumption by monitoring the current drawn from all devices on the same node. Furthermore, the power source of the Energy Source can be recharged by connecting several Energy Harvesters.

The Energy Source base class includes Device Energy Model objects and Energy Harvester objects that obtain power. If the Energy Source runs out of control, it notifies

all devices on its list. Each node can react appropriately and follow the prescribed protocol during a power disaster.

### 2) Device energy model

Measures a device's energy consumption by assigning power values to its different states. When the device changes conditions, the Energy Source is notified and recalculates the total power draw. This model can work for devices with infinite states, like an electric vehicle's motor, by directly converting speed values to current.

### 3) Energy harvester

When recharging the Energy Source, it's important to consider both the energy output of the environment and the efficiency and power consumption of the Energy Harvester. The Energy Harvester collects energy from the surroundings, making it a valuable tool for energy collection.

### C. Packet Delivery Ratio (PDR)

When assessing a sensor network's effectiveness, it's typical to gauge the number of packets the server receives relative to the number of packets dispatched by the end nodes. This measurement, referred to as PDR, can be computed either node by node or for the entire network. For the latter, Eq. (6) is the appropriate calculation.

$$PDR = \frac{\sum \text{Number of packet received}}{\sum \text{Number of packet sent}} \quad (6)$$

### D. Delay (Second)

The Delay is measured from when the packet leaves the source application to when the same packet arrives at the destination application.

$$\text{Delay} = \frac{\sum(\text{TPR}-\text{TPT})}{\text{Number of Packets Received}} \quad (7)$$

where,

T P R = Time Packet Received.

T P T = Time Packet Transmitted.

## III. SIMILAR WORKS

Many researchers conduct interesting studies and papers on improving the performances of the Internet of Mobile Things by employing various techniques.

Following is a list of various works in this field: Wu *et al.* [10] provided a general model that uses a state machine to estimate energy usage in LoRaWAN for various channel access techniques. They can characterize the energy usage for particular access mechanisms or the entire network. According to this model, random access only operates at peak efficiency when no further receive windows are opened. Listening before speaking is an easy improvement. Advantages are made for networks with high loads using a more complicated schedule.

Loh *et al.* [11] presented a contribution to enhancing the Adaptive Data Rate (ADR) in the case of predefined mobility patterns. By incorporating the positional information and trajectories of mobile devices for dynamic

allocation, the proposed Enhanced-ADR (E-ADR) approach aims to optimize transmission time, energy consumption, and packet loss for mobile devices. In [12], the same authors extend E-ADR to unknown mobility patterns. In the case when sensors travel with unknown or undefined trajectories. This extension, called the Variable Order Hidden Markov Model (VHMM), is based on E-ADR to predict the node trajectory.

Benkahlia *et al.* [13] put forth two ADR proposals that will be managed by Network Server NS, the Gaussian filter-based ADR (G-ADR) and the Exponential Moving Average-based ADR (EMA-ADR). Both of these methods function as a low-pass filter, intending to resist sudden changes in the signal-to-noise ratio of received packets at the NS. Their proposed approaches are geared towards allocating the most suitable Spread Factor SF and Transmit Power TP to mobile and static EDs, aiming to reduce convergence time in the confirmed mode of LoRaWAN.

Like [14], the authors employed simulation tools to demonstrate that the movement of end devices results in invalid configuration commands for setting the spreading factor and the transmission power for an end device. Recently [15], the distance between the ED's former and present positions at the NS is used by the proposed Mobility ADR (M-ADR) to determine the ED status (i.e., whether it is static or movable). They employed the Kalman Filter to estimate the Signal-to-Noise Ratio (SNR) to precisely determine SF, TP, or both if the ED status was found to be mobile because these parameters are primarily dependent on SNR. The suggested M-ADR further determines the ideal SF and TP configuration after the Kalman Filter determines the system's current estimate.

To evaluate the network performance and energy consumption, Farhad *et al.* [16] have simulated LoRaWAN-Aloha and LoRaWAN-CSMA/CA under various networking scenarios by varying network load, spreading factors, and sensor and gateway distances. The simulation's findings compare and contrast CSMA and Aloha regarding collision rate, the likelihood that a network would succeed, and energy usage per node. According to the performance analysis, LoRaWAN-CSMA/CA may be a better option than LoRaWAN-Aloha for large IoT networks with stringent scalability requirements. But for a small, static IoT network, LoRaWAN Aloha might be a better option.

In [17], they enable the analysis of LoRa in terms of energy efficiency by modeling the energy consumption of the SX1272, a standard LoRa chip. They perform real-world measurements of the chip to develop a device profile and use the results to create an energy consumption module in ns-3 to evaluate LoRa networks in terms of energy efficiency.

Finnegan *et al.* [18] suggested slotted CAD to maintain 100% PDR and experimental 4800 bps data throughput without other environmental disturbances. Compared to different scenarios, the proposed slotted CAD CSMA/CA approach efficiently uses the free channel and avoids collisions while minimizing delay time.

#### IV. RESULTS AND DISCUSSIONS

This section presents the results of different simulation scenarios by varying the number of end devices, sending periods, number of gateways, packet size, and radius. These results are analyzed and evaluated to study the impact of different mobility models on energy remaining, PDR, and delay in Lora Networks.

The simulation goes up to 50, 100, 300, and 500 ED with 1 and 2 GW, the simulation time equals 3600s (1 hour), and a power source: a 200 mAh battery. The node sends data frames to the GW (uplink) with a size of 12 bytes every 5 seconds. The ED positions are randomly assigned around the GW in a radius of 1000, 5000, 8000, 10000, and 15000 meters; a simulator of an energy recuperator is added, which periodically collects a random value. The remaining energy is evaluated, and their effectiveness is compared using the NS-3 simulator; the Lora network is simulated by increasing the number of nodes for the three mobility models.

TABLE I: SIMULATION PARAMETERS.

| Parameters       | Value                                | Unit     |
|------------------|--------------------------------------|----------|
| N of Nodes       | 50, 100, 300, 500                    | -        |
| Radius           | 1000, 5000, 8000, 10000, 15000       | Meter    |
| Period           | 3, 5, 7                              | Second   |
| Packet Size      | 12, 64, 120, 192, 216                | Byte     |
| Gateway (GW)     | 1, 2                                 | -        |
| Simulation Time  | 3600                                 | Second   |
| Mobility Model   | <b>ConstantPositionMobilityModel</b> | -        |
| -                | <b>RandomWayPointMobilityModel</b>   | -        |
| -                | Vitesse Max = 60                     | meters/s |
| -                | Pause Time = 0                       | second   |
| -                | <b>GaussMarkovMobilityModel</b>      | -        |
| -                | Vitesse Min=20, Max = 70             | meters/s |
| -                | Pause Time = 2, $\alpha = 1$         | -        |
| Energy Initial   | 200                                  | mAh      |
| Battery PD2032   | 2664                                 | Joules   |
| -                | 3.7                                  | Volts    |
| Simulator        | NS3 (Version 3.35)                   | -        |
| Operating System | Ubuntu 24.4 64bit                    | -        |

Fig. 7 below presents the energy remaining as a function of the simulation time equal to 3600 sec in four (04) scenarios with three mobility models. The impact of the mobility model on the remaining energy is essential. When 1 ED (end device) sends a packet of size 12 bytes every 05 seconds within a radius of 20m around a single GW (Fig. 7. (a)), the second case is with two GW (Fig. 7. (b)), the third case with 500 ED and one GW (Fig. 7. (c)), and finally, with 500 ED and a packet size of 24 bytes and one GW (Fig. 7. (d)); energy remaining decreases during the simulation time for all four scenarios.

In the first scenario, the GM mobility model with  $\alpha = 1$ , pause time = 2 seconds and a speed varying between 20 and 70 m/s performs better than the two other models with an energy remaining of 2663.9 J. This is because consumption during one hour (simulation time) equals 0.1J. For the two rest models, RWP and CP, the energy consumption is 0.4J, which equals 9.6J in 24h, making the GM model 4 times less than the RWP and CP models. In the second scenario, when adding a second The GM mobility model also gives good results compared

to the two other models but performs less than the first scenarios. In the third scenario, when increasing the number of ED to 500 nodes. CP and GM have the same value of 2663.6J, while the worst model is RWP, with a max speed of 60 m/s. In the fourth and last scenario, notice that the GM model has been slightly impacted by the packet size when it is increased by energy remaining of

2663.2J, while the CP model is better performing with a value of 2663.6J. The worst model is the RWP of the time pause, which is zero, i.e., maximum mobility.

As already seen in the preceding sections, the impact of the mobility model on residual energy, node density, PDR (%), and latency is the primary emphasis of this work (see Fig.7).

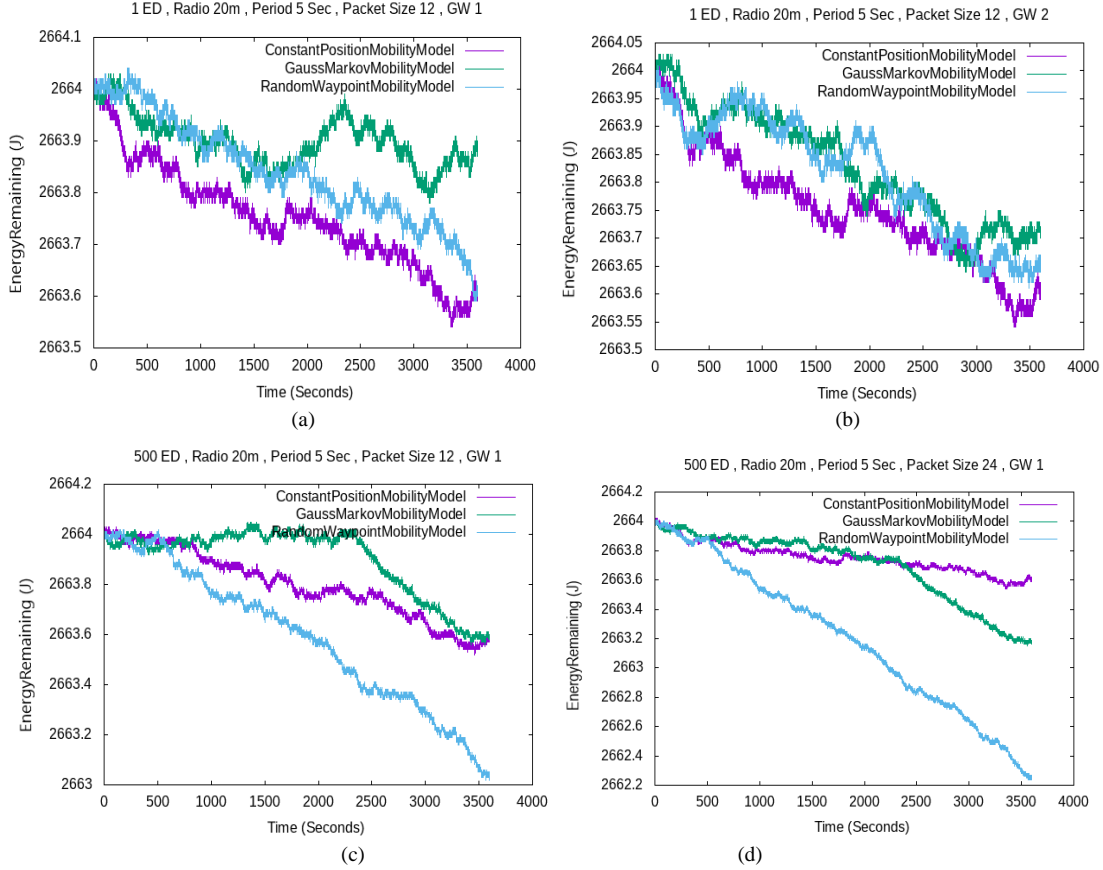


Fig. 7. Impact of mobility model on energy remaining. (a)One End device and Gateway, (b)Two Gateway and one device (C)500 ED and Packet size 12(d) 500 ED and Packet size 24.

TABLE II. SIMULATION VALUES

| Mobility Model          | ED  | Packets Sent | Packets Received | PDR (%) | Packets Loss | Total Delay (Sec) |
|-------------------------|-----|--------------|------------------|---------|--------------|-------------------|
| Constant Position Model | 01  | 618          | 618              | 100     | 00           | 0.37070           |
|                         | 50  | 30874        | 25697            | 83.23   | 5177         | 0.13766           |
|                         | 100 | 61736        | 41549            | 67.30   | 20187        | 0.10645           |
|                         | 300 | 185222       | 58530            | 31.59   | 126692       | 0.09096           |
|                         | 500 | 308708       | 49847            | 16.14   | 258861       | 0.07899           |
| Random WayPoint Model   | 01  | 618          | 618              | 100     | 00           | 0.05657           |
|                         | 50  | 30874        | 23628            | 76.53   | 7246         | 0.05657           |
|                         | 100 | 61745        | 42326            | 68.54   | 19419        | 0.05657           |
|                         | 300 | 185234       | 57989            | 31.30   | 127245       | 0.05657           |
|                         | 500 | 308695       | 51303            | 16.61   | 257392       | 0.05657           |
| Gauss Markov Mobility   | 01  | 618          | 618              | 100     | 00           | 0.05657           |
|                         | 50  | 30875        | 24587            | 79.63   | 6288         | 0.13337           |
|                         | 100 | 61740        | 40326            | 65.31   | 21414        | 0.05657           |
|                         | 300 | 185215       | 61936            | 33.44   | 123279       | 0.05657           |
|                         | 500 | 308705       | 53385            | 17.29   | 255320       | 0.05657           |

The packet delivery ratio is shown in Fig. 8(a) below as a function of the number of nodes. PDR is the ratio of packets delivered to the total number of packets generated. The PDR is inversely correlated to the packet loss rate. A higher packet delivery rate means less packet loss. When there are more nodes in the network, there are more collisions, which causes the PDR to decrease. At 500 ED in a 20-meter radius around the GW, the graph shows almost the same performances as the three mobility models. The PDR decreases with an increase in the ED by less than 20% since collisions during transmission are less frequent when the number of ED is lower and the collisions increase.

They are keeping the same simulation parameters, except the distance increase between ED and GW to 8000 meters, as shown in Fig. 8 (b). CP and GM provide a PDR greater than 50%, but RWP provides the worst PDR of always less than 20%.

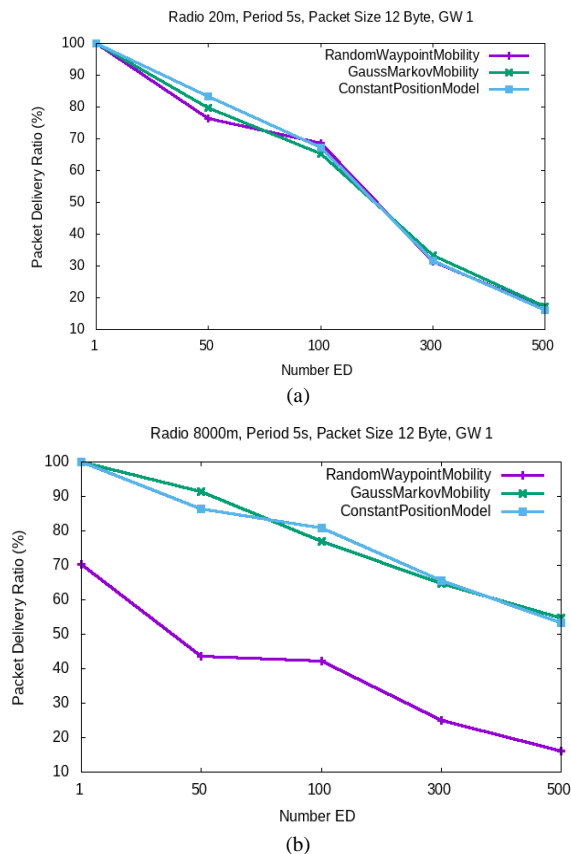


Fig. 8. Impact of number ED on PDR, (a) PDR Vs Number ED with radius=20m, (b) PDR Vs Number ED with radius=8000m.

Fig. 9 (a) shows the PDR as a function of radius and follows the same behavior as the number of nodes. When the radius increases, it leads to a decrease in the PDR. With 10 ED. GM marks good results when showing a percentage of 80%, CP slightly less than 70%; unlike the first two, poor results are presented by the RWP, from 8000 m is a decrease of less than 50%, and at 15000 m is at 20%.

In Fig. 9 (b), by increasing the number of EDs to 300 nodes, the result PDR is less than the PDR in graph 9 (a), seen at the increase in the number of collisions, but greater than 50% for GM and CP model, and still, RWP continues

to be the worst model when it marks a PDR between 10% and 20%.

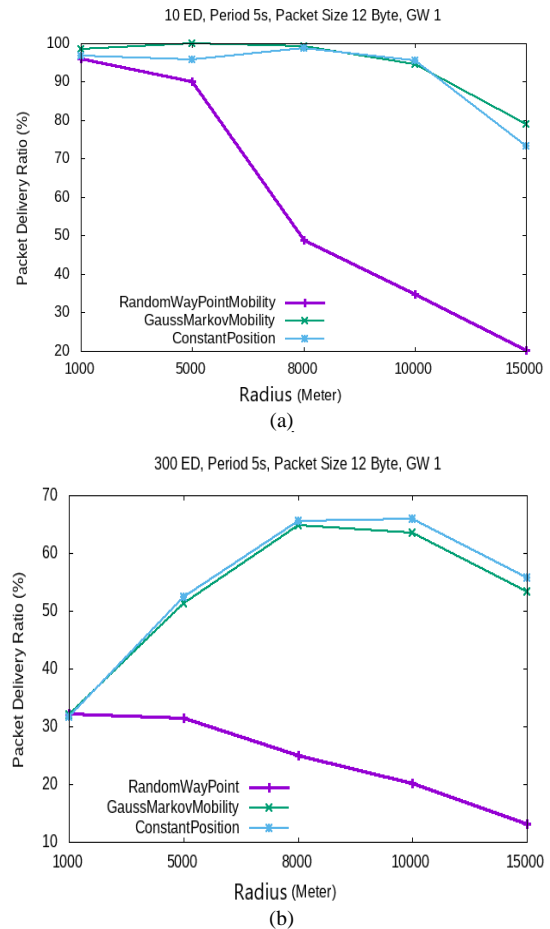


Fig. 9. Impact of radius on PDR, (a) PDR Vs Radius With 10 ED, (b) PDR Vs Radius with 300ED.

In Fig. 10, the graph shows the effect of increasing the radius of the area on the end-to-end delay for 300 ED and one gateway; notice that the uncertainty remains constant for the three mobility models in a radius between 100 and 1000 meters, with a delay value of less than 0.06 seconds. As soon as the distance increases from 1000 meters to 15000 meters, the GM and CP models increase linearly until 0.13 seconds. The RWP model remains almost constant, keeping the same value between 0.05 and 0.06 seconds throughout the simulation, despite increasing the radius to 15000 meters.

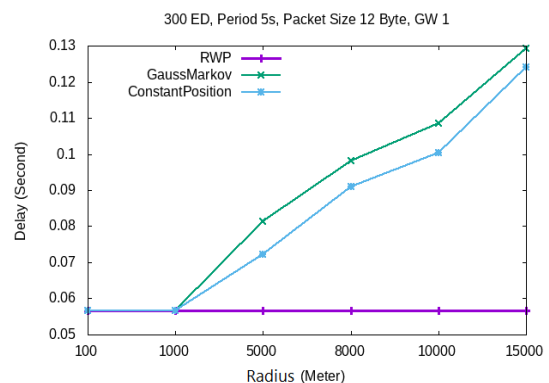


Fig. 10. Delay VS radius.

The Fig. 11 below shows the delay as a function of the number of nodes. Within a radius of 8000 meters, the delay increases with the number of nodes in the network. The nodes send data frames; collisions and interferences appear more frequently in this case. The delay increases steadily for the GM and CP models, up to 160 seconds for 500 ed. The delay also increases slightly for the RWP, which is less than 20 seconds.

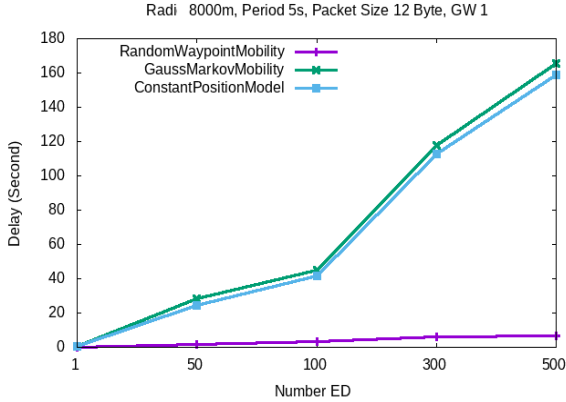


Fig. 11. Delay VS Number ED.

Fig. 12 shows how changing the packet size from 12 to 216 bytes affects the PDR. It is observed that the PDR decreases constantly with increasing the packet size for the three mobility models. With 50 E D and one gateway, a transmission interval of 5 seconds in a range of 20 m can reach a PDR between 75 to 85% with a small payload (12 bytes), keeping the same parameters but increasing the packet size to 216 bytes, the PDR decreases to 30%.

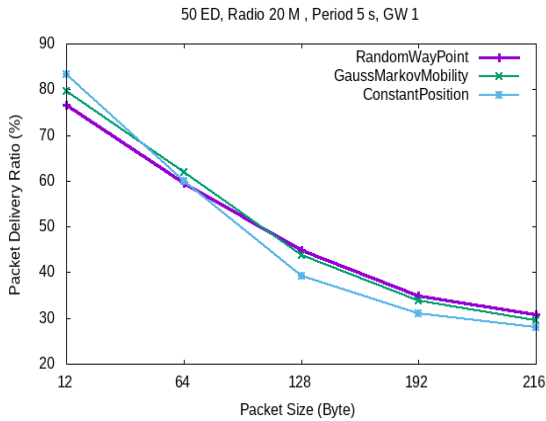


Fig. 12. PDR Vs packet size.

**A. Alpha Value**

In all the above graphs, the GM mobility model uses Alpha = 1, as shown in Table I; the following chart shows the results when Alpha = 0.5 to notice the random variable's impact better.

The PDR is represented in Fig.13 below as a function of the number of nodes up to 500 ED, around 20 meters from the gateway. Comparing with Fig.8 (a) (same simulation parameter used), except that the GM mobility model has changed the value of Alpha = 0.5 instead of 1, which clearly shows the impact of Alpha on the result obtained.

With Alpha = 0.5, the GM model performs better than with Alpha =1. In Fig.8 (a), the PDR is less than 20% for the three mobility models, while with Alpha = 0.5 relative to the GM model, the PDR is greater than 50%, as illustrated in Fig. 13.

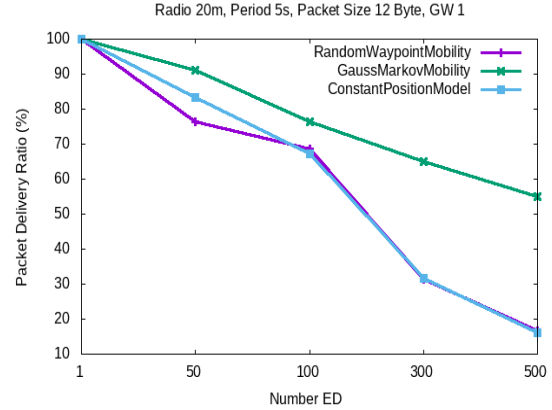


Fig. 13. PDR Vs. Number ED With Alpha = 0.5.

**B. Energy Harvester**

Fig. 14 shows the evolution of the remaining energy in the end node during the simulation time, where energy recovery mitigates the energy expenditure associated with sending packets when the sending period is longer than 5 seconds (exactly 7 seconds) using the recovery module.

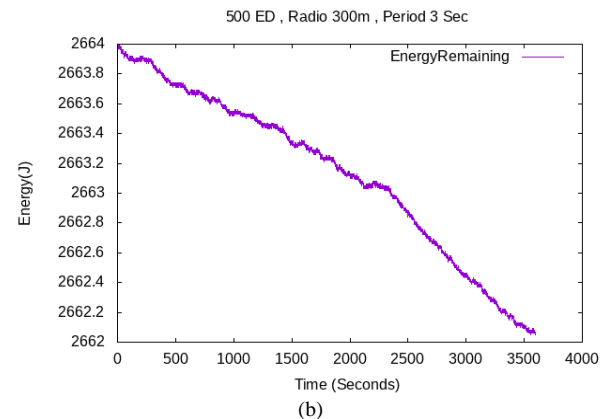
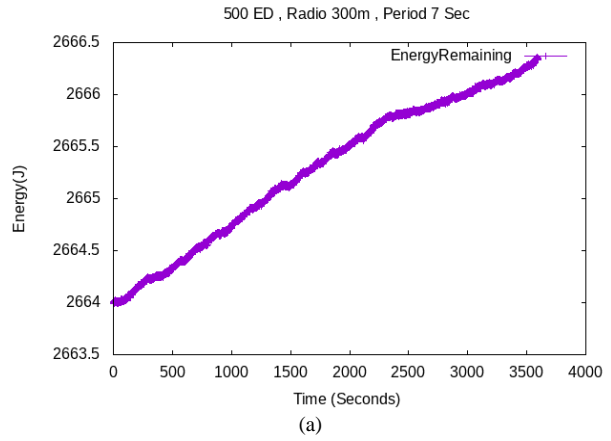


Fig. 14. Impact of Period Send on Energy Remaining. (a) Period send packet > 5s. (b) Period send packet < 5s;

But when the sending period is less than 5 seconds (3 seconds), Fig.14(b) shows the impact of the transmission speed on the energy recovery module and that the remaining energy is not constantly replenished.

TABLE III. MEASUREMENT CONFIGURATION.

| Parameters          | Value      |
|---------------------|------------|
| Transmit Power (TP) | 14 dBm     |
| Frequency           | 433 Mhz    |
| Bandwidth           | 125 kHz    |
| Packet Length       | 12 Byte    |
| Period Send         | 05 second  |
| Baud                | 115200 bps |

V. EXPERIMENTS AND RESULTS

In this section, this study describes the experimental setup evaluation metrics and presents the results of the experience. The experiment uses the Cube Cell HTCC-AB01 module based on ASR605x chips, which operates at 433, 868, and 915 MHz; a lot of migration and development has been done to make it perfectly support Arduino® to run the LoRaWAN protocol correctly and can easily connect lithium, batteries, and solar panels with a maximum transmission power of 22 dBm. These modules are provided by Heltec Automation [19]. The measuring system, which consists of two LoRa Cube Cell HTCC-AB01 modules and two computers, is depicted in Fig. 15(a). As seen in Fig.15(b), a LoRa module is linked to a computer via a serial interface that can enable half-duplex communication and is powered by a laptop. Data packets are sent or received by the system’s computers while operational and transmitted between two Cube Cell HTCC-AB01 modules through a radio link. Experience can evaluate the transmission efficiency using the measured packets.

During the experiment, the LoRa transmitter continuously sends packets of 12 bytes every 05 seconds, using two (02) Cube Cell HTCC-Ab01 powered by Laptop one is considered as Sender fixed on the car’s roof with a height of 150 Cm from the ground level as shown on Fig. 15(b). The second module represents a receiver node; it is mobile because it is placed inside the vehicle and moves at a speed between 20-70 m/s. LoRa node is set to point-to-point (P2P) transmission mode with a transmit power of 14 dBm and a 2.5 dBi gain antenna. The carrier frequency is

433 MHz, and the bandwidth is 125 kHz. The baud rate of the serial interface is set to the maximum value of 115200 bps. The parameters used are illustrated in Table III.

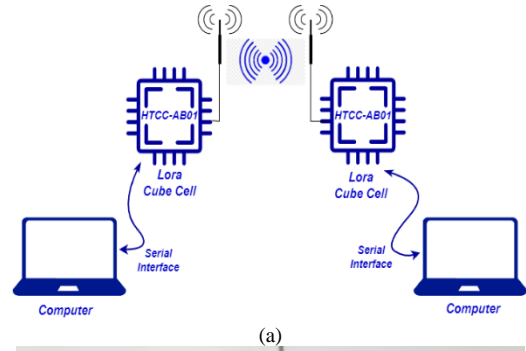


Fig. 15. (a)Architecture of measurement system, (b), Measurement System.

Finding a test site for long-range LoRa radio communications was very difficult. Two (02) sites were recommended, the first in the city center of the wilaya of Chlef in Algeria, in an urban area at coordinates 36.1590687 and 1.3239960; this is the most difficult in terms of transmission reliability because of high buildings, trees, congested areas, and narrow streets. The experiment is conducted at 23:30. Experience indicates that the maximum distance obtained is 966.97 meters of a line sight, as shown in Fig. 16.



Fig. 16. Distance traveled in an urban area.

Google Maps Fig. 16 demonstrates that while the transmitter stays in its initial location and does not move during the measurement procedure, the receiver position continues to move until it reaches the farthest point of 966.97 meters of line of sight.

Fig. 17 shows the experimental Received Signal Strength Indicator (RSSI) about the distance traveled in meters. The measurement of signal reception at the receiver, indicated by the value of the radio signal strength (RSSI), shows a trend that continues to decrease with increasing distance. This is consistent with the nature of long-distance communication transmission, i.e., the signal strength will weaken as the distance between transmitter and receiver increases.

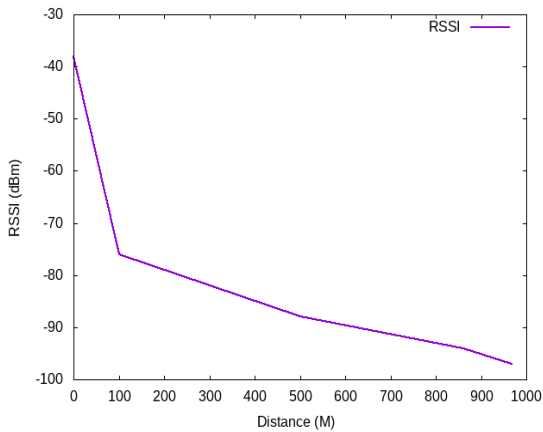


Fig. 17. RSSI (dBm) vs distance (M) in an urban area.

The Fig.18 displays the number of lost packets about distance. A linear increase in incorrect and rejected packets

is affected by interferences, and since the Lora receiver module is mobile, remoteness from the transmitter module will be followed by a decrease in signal strength.

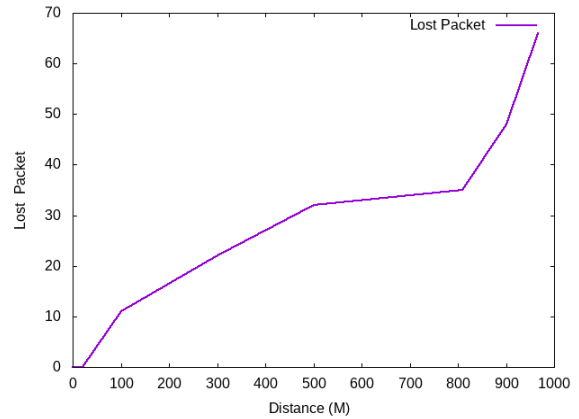


Fig. 18. Lost Packet vs Distance (M) in an urban area.

The second experiment was conducted in an open field in a rural area with fewer obstacles at coordinates 36,248,630,9, 13,319,770. With the same parameters, the receiver module moves until it reaches the furthest distance. The location map from Google Maps and the measurement points are shown in Fig. 19. Experience indicates that the maximum length obtained is 1,310 meters of the line of sight.

Fig.20 shows the RSSI about the distance traveled in meters. RSSI decreases with increasing distance. The signal strength measurement at the receiver is indicated by the lowest RSSI value of  $-98$  dBm, and the highest RSSI value of  $-37$  dBm. The impact of distance on signal strength is clearly illustrated.



Fig. 19. Distance traveled in a rural area.

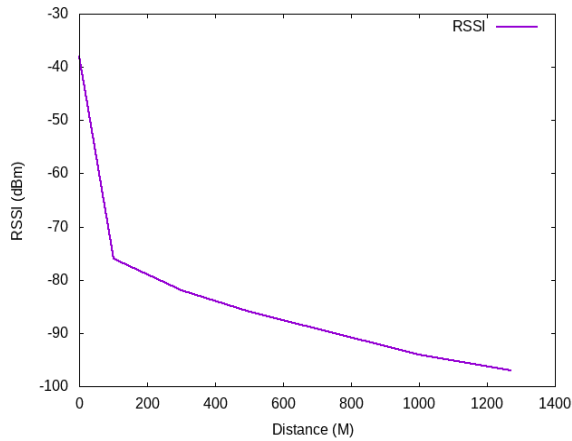


Fig. 20. RSSI (dBm) vs Distance (M) in a rural area.

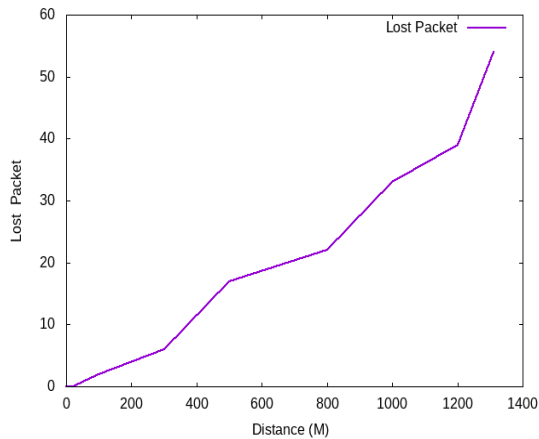


Fig. 21. Lost Packet vs Distance (M) in a rural area.

The number of lost packets about the distance is shown in Fig.21. The graph shows a linear increase in lost packets—a high RSSI results in low packet loss. However, packet loss becomes evident when RSSI falls below -90 dBm and increases rapidly as RSSI decreases. RSSI is impacted by distance, and consequently the number of lost packets is affected by RSSI.

## VI. CONCLUSION

This paper examines the impact of mobility models on LoraWan performance using both NS3 simulations and real-world experiments across various scenarios. This research examines a comprehensive evaluation of the top three frequently employed mobility models in academic circles: Random Way Point (RWP), Gauss Markov (GM), and Constant Position (CP) Model. The performances are analyzed using different metrics (delay, packet delivery ratio, energy remaining, packet size, radius, and number of nodes). The simulation results indicate that the GM model performs well regarding energy consumption and radius; the GM model with Alpha = 1 performs better than the other two models, and Alpha = 0.5 performs even better in terms of PDR. At the same time, the RWP demonstrates positive results regarding delays. In studying protocols or applications that utilize LoRaWAN, it is imperative to consider the relevant mobility parameters. This consideration is crucial for ensuring the efficiency and reliability of the system, as well as for optimizing its

overall performance. Therefore, it is recommended that researchers and industrials alike give due attention to this critical aspect of LoRaWAN-based systems. Experiments conducted with the Cube Cell HTCC-AB01 indicate network performance matches simulations, particularly in rural areas. In forthcoming times, there will be an emphasis on examining a greater number of radio elements and parameters, with a particular focus on the interference that may arise between different networks.

## CONFLICT OF INTEREST

The authors declare no conflict of interest.

## AUTHOR CONTRIBUTIONS

Abdelouahab Nouar analyzed simulation results and wrote the paper; Mounir TAHAR ABBES contributed by guiding, giving directions and also wrote the paper; Mostefa Chaib prepared and analyzed experiments results; Selma Boumerdassi proofread and correcting errors. All authors had approved the final version.

## REFERENCES

- [1] Lorawan academy, what are lora® and lorawan. [Online]. Available: <https://tech-journal.semtech.com/understanding-the-lorawan-architecture> (accessed on 23 March 2023).
- [2] Adaptive data rate. [Online]. Available: <https://www.thethingsnetwork.org/docs/lorawan/adaptive-data-rate/>
- [3] S. Umbreen, D. Shehzad, N. Shafi, B. Khan, and U. Habib, "An energy-efficient mobility-based cluster head selection for lifetime enhancement of wireless sensor networks," *IEEE Access*, vol. 8, pp. 207–779, 2020.
- [4] D. B. Johnson and D. A. Maltz, "Dynamic source routing in ad hoc wireless networks," pp. 153–181, 1996.
- [5] Dynamic Source Routing in Ad Hoc Wireless Networks. [Online]. Available: [https://doi.org/10.1007/978-0-585-29603-6\\_5](https://doi.org/10.1007/978-0-585-29603-6_5)
- [6] F. Geng and S. Xue, "A comparative study of mobility models in the performance evaluation of MCL," in *Proc. 2013 22nd Wireless and Optical Communication Conference*, 2013, pp. 288–292.
- [7] A. B. Yagouta, M. Jabberi, and B. B. Gouissem, "Impact of sink mobility on quality-of-service performance and energy consumption in a wireless sensor network with cluster-based routing protocols," in *Proc. 2017 IEEE/ACS 14th International Conference on Computer Systems and Applications (AICCSA)*, 2017, pp. 1125–1132.
- [8] D. Magrin, M. Centenaro, and L. Vangelista, "Performance evaluation of Lora networks in a smart city scenario," in *Proc. 2017 IEEE International Conference on Communications (ICC)*, 2017, pp. 1–7.
- [9] Network simulator (ns)-3. [Online]. Available: <https://www.nsnam.org/> (accessed on 23 march 2023).
- [10] H. K. Wu, S. Nabar, and R. Poovendran, "An energy framework for the network simulator 3 (ns-3)," in *Proc. International ICST Conference on Simulation Tools and Techniques*, 2011.
- [11] F. Loh, S. Raffek, S. Geißler, and T. Hofbeld, "Generic model to quantify energy consumption for different lorawan channel access methods," in *Proc. 2022 18th International Conference on Wireless and Mobile Computing, Networking, and communications (WiMob)*, 2022, pp. 290–295.
- [12] N. Benkahla, H. Tounsi, Y. Q. Song, and M. Frikha, "En-hanced adr for lorawan networks with mobility," in *Proc. 2019 15th International Wireless Communications Mobile Computing Conference (IWCMC)*, 2019, pp. 1–6.
- [13] N. Benkahla, H. Tounsi, Y.-Q. Song, and M. Frikha, "Vhmm-based e-adr for lorawan networks with unknown mobility patterns," in *Proc. 2021 International Wireless Communications and Mobile Computing (IWCMC)*, 2021, pp. 86–91.

- [14] A. Farhad, D. H. Kim, S. Subedi, and J. Y. Pyun, "Enhanced Lorawan adaptive data rate for mobile internet of things devices," *Sensors*, vol. 20, no. 22, 2020.
- [15] A. Farhad, D.-H. Kim, B.-H. Kim, A. F. Y. Mohammed, and J. Y. Pyun, "Mobility-aware resource assignment to IoT applications in long-range wide area networks," *IEEE Access*, vol. 8, pp. 186 111–186 124, 2020.
- [16] A. Farhad, G.-R. Kwon, and J.-Y. Pyun, "Mobility adaptive data rate based on Kalman filter for lora-empowered iot applications," in *Proc. 2023 IEEE 20th Consumer Communications Networking Conference (CCNC)*, 2023, pp. 321–324.
- [17] M. Baddula, B. Ray, and M. Chowdhury, "Performance evaluation of Aloha and csma for Lorawan network," in *Proc. 2020 IEEE Asia-Pacific Conference on Computer Science and Data Engineering (CSDE)*, 2020, pp. 1–6.
- [18] J. Finnegan, S. Brown, and R. Farrell, "Modeling the energy consumption of lorawan in ns-3 based on real-world measurements," in *Proc. 2018 Global Information Infrastructure and Networking Symposium (GIIS)*, 2018, pp.1–4.
- [19] M. H. Tsoi, T. H. Ng, D. P. K. Lun, Y. S. Choy, and S. W. Y. Mung, "Lora data throughput enhancement by slotted channel activity detection," in *Proc. 2020 IEEE Asia-Pacific Microwave Conference (APMC)*, 2020, pp. 466–468.
- [20] Cubecell. [Online]. Available: <https://www.heltec.org>

Copyright © 2024 by the authors. This is an open-access article distributed under the Creative Commons Attribution License ([CC BY-NC-ND 4.0](https://creativecommons.org/licenses/by-nc-nd/4.0/)), which permits use, distribution, and reproduction in any medium, provided that the article is properly cited, the use is non-commercial and no modifications or adaptations are made.